

UC Irvine

UC Irvine Previously Published Works

Title

Engineering Densely Packed Arrays of Rare Earth Silicide Nanowires on Si(001)

Permalink

<https://escholarship.org/uc/item/9pf249tz>

Authors

Ragan, Regina

Chen, Yong

Ohlberg, Douglas AA

et al.

Publication Date

2003

DOI

10.1109/nano.2003.1231752

Copyright Information

This work is made available under the terms of a Creative Commons Attribution License, available at <https://creativecommons.org/licenses/by/4.0/>

Peer reviewed

Engineering Densely Packed Arrays of Rare Earth Silicide Nanowires on Si(001)

Regina Ragan, Yong Chen, Douglas A.A. Ohlberg,
and R. Stanley Williams
^aQuantum Science Research
Hewlett-Packard Laboratories
Palo Alto, CA USA
regina.ragan@hp.com

Jianhua Yang, and Y. Austin Chang
Material Science and Engineering
Univ. of Wisconsin at Madison
Madison, WI USA

Abstract— Ordered arrays of self-assembled ErSi_{2-x} , SmSi_{2-x} , DySi_{2-x} and HoSi_{2-x} nanowires aligned along Si [110] have been grown at 600°C on Si(001) vicinal substrates with wire widths on the order of a nanometer and lengths exceeding 1 micron. The nanowires were characterized *in situ* with scanning tunneling microscopy and *ex situ* with atomic force microscopy. The length of coherently strained nanowires is dependent on surface kinetics while the wire width is thermodynamically controlled via strain energy. The unit cell of these rare earth disilicides is non-cubic and has an asymmetric lattice mismatch with the cubic unit cell of Si. The nanowire width decreases monotonically with increasing lattice mismatch between the Si $[\bar{1}10]$ and RSi_{2-x} [0001] lattice constants. Therefore, nanowire width may be varied by tuning the RSi_{2-x} lattice constant along [0001] via fabrication of a ternary disilicide. In addition, the crystal quality of the nanowires may be improved by minimizing the lattice mismatch along the wire axis. We have grown $(\text{Er}_{1-y}\text{Ho}_y)\text{Si}_{2-x}$ and $(\text{Er}_{1-y}\text{Dy}_y)\text{Si}_{2-x}$ nanowires on Si(001) and analyzed the microstructure to investigate ternary disilicide growth.

Keywords—component; A1. Low dimensional structures; A1. Asymmetric lattice mismatch; A3. Physical vapor deposition; A3. Self assembled nanowires; B1. Rare earth silicides

I. INTRODUCTION

One of the primary goals in the material science of nanostructures is the fabrication of ordered arrays of quantum structures with uniform size and shape in a scalable process. While lithographic techniques are technologically highly developed, lithography may be disadvantageous in terms of high cost, low throughput or both for the fabrication of nanostructures on the nanometer length scale. Self-assembly of nanostructures has been demonstrated in many systems. The Langmuir-Blodgett and self-assembled monolayer techniques produce ordered molecular films and various epitaxial and atomic layer deposition techniques produce organic and inorganic quantum dots and wires. The exploitation of self-assembly for device fabrication is contingent on the ability to control the size and shape of these quantum structures and thereby engineer the desired electronic and/or optical properties. In order to fabricate ordered arrays of nanostructures, there is a need to investigate both

experimentally and theoretically the thermodynamic and kinetic driving forces in these systems.

Self-assembled rare earth disilicide (RSi_{2-x} , with $x \sim 0.30$)[1] nanowires on Si(001) are an interesting system to study strain driven, epitaxial nanocrystals formation. Since thin films of RSi_{2-x} demonstrate metallic behavior and form contacts to n-type Si with a low Schottky barrier, these nanowires may have applications as non-lithographically fabricated interconnects with feature sizes on the order of a nm. Due to the narrow width, RSi_{2-x} nanowires may also serve as etch masks for non-lithographic Si nanowire fabrication. In addition, one-dimensional structures may exhibit interesting phenomenon such as a Peierls transition [2] and Luttinger liquid behavior [3]; hence, characterization of RSi_{2-x} nanowires may lead to a deeper fundamental understanding of the physical properties of one-dimensional structures.

DySi_{2-x} was the first RSi_{2-x} observed to self-assemble into nanowires on Si(001) although the self-assembly mechanism was not understood.[4] Since then many RSi_{2-x} (for example, $R = \text{Er, Ho, Gd, Sc, and Sm}$) with the hexagonal AlB_2 crystal structure have been demonstrated to self-assemble into nanowires during epitaxial growth on Si(001).[4-8] The evolution of the one-dimensional structure during epitaxial growth on Si(001) was attributed to an anisotropic lattice mismatch between the [0001] and $[\bar{1}1\bar{2}0]$ lattice constants of the RSi_{2-x} and the Si [110] lattice constant, $a_{\text{Si},[\bar{1}10]}$. [5] For example, the lattice mismatch between ErSi_{2-x} [0001] $\{[\bar{1}1\bar{2}0]\}$ and Si $[\bar{1}10]$ $\{\text{Si}[110]\}$ is 6.3% $\{-1.6\%$. The RSi_{2-x} grows preferentially in the direction that has the small lattice mismatch with $a_{\text{Si},[\bar{1}10]}$ and growth is constrained in the large lattice mismatch direction, thus, forming nanowires. Two orientations of nanowires grow on ‘flat’ Si(001) substrates with the long axes of the nanowires orthogonal to one another and perpendicular to the Si dimer rows. ‘Flat’ Si(001) substrates with a miscut $< 2^\circ$ have single atomic steps and the terraces alternate between dimer rows running parallel (type A) and perpendicular (type B) to the step edge. The alignment of ErSi_{2-x} , SmSi_{2-x} and DySi_{2-x} nanowires along a single direction was achieved by growth on vicinal Si(001) substrates.[8] The

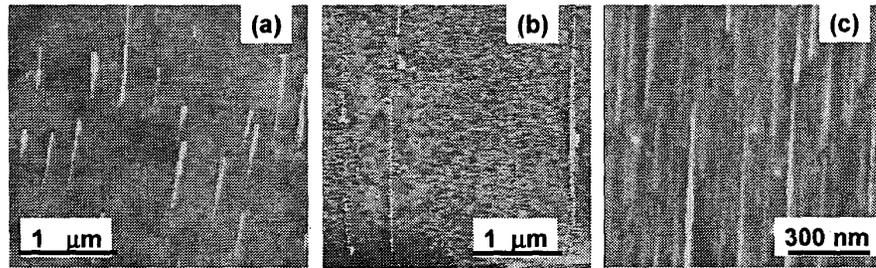


Figure 1: AFM images of HoSi_{2-x} nanowires grown on vicinal $\text{Si}(001)$ substrates with a miscut of 2.5° toward $[110]$. The RSi_{2-x} nanowire arrays are oriented along the $\text{Si} [110]$ direction. The growth rate and coverage are (a) 0.15 ML/min and 0.15 ML, (b) 0.025 ML/min and 0.05 ML and (c) 0.05 ML/min and 0.35 ML.

2×1 reconstructed $\text{Si}(001)$ vicinal surface with a miscut of 2.5° toward $[110]$ has double atomic steps of type B. Hence, aligned arrays of RSi_{2-x} nanowires grow perpendicular to the dimer rows and parallel to the step edges. Aligned, dislocation-free nanowire arrays having a high density and uniform wire width are desirable for interconnects and for use as an etching template. Here we report the dependence of nanowire length and density on incoming flux. In addition, the nanowire width is shown to decrease with increasing lattice mismatch between $[0001]$ and $\text{Si} [\bar{1}10]$ as shown in previous work.[6] Therefore, the fabrication of ternary disilicides $\{(\text{R}_{1-y}\text{R}^*_y)\text{Si}_{2-x}\}$ with the large lattice mismatch tuned as a function of alloy composition (y) may enable engineering of nanowire width. As an additional constraint, the small lattice mismatch between $a_{\text{Si}[\bar{1}10]}$ and $(\text{R}_{1-y}\text{R}^*_y)\text{Si}_{2-x} [11\bar{2}0]$ should be minimized for dislocation-free nanowire growth along the wire axis. We have grown both $(\text{Er}_{1-y}\text{Ho}_y)\text{Si}_{2-x}$ and $(\text{Er}_{1-y}\text{Dy}_y)\text{Si}_{2-x}$ nanowires on vicinal $\text{Si}(001)$ substrates and analyzed with atomic force microscopy (AFM), scanning tunneling microscopy (STM) and Auger electron spectroscopy (AES).

II. EXPERIMENT

$\text{Si}(001)$ vicinal substrates with a miscut of 2.5° toward $[110]$ were prepared by heating the substrate to a temperature of 1150°C for 15 seconds in ultrahigh vacuum with a chamber pressure $< 1 \times 10^{-9}$ Torr. The $\text{Si}(001)$ surface was analyzed *in situ* with a STM to ensure a clean 2×1 reconstructed surface prior to deposition. Physical vapor deposition of rare earth metals was performed via an electron beam evaporator. For ternary rare earth disilicide nanowire growth, the e-beam evaporator was filled with a solid solution of two rare earth metals. These binary solid solutions were prepared by arc melting appropriate ratios of high purity starting materials.[9] The growth rate of the rare earth metal was varied from 0.02 - 0.15 monolayer (ML)/min to determine the dependence of nanowire length on incoming flux. The substrate temperature during deposition was held constant at 600°C . The sample was annealed post-growth at 600°C to drive the reaction between the rare earth element and Si to completion. The nanowires were characterized *in situ* with an Omicron STM with a chamber pressure $< 2 \times 10^{-10}$ Torr and *ex situ* with AFM.

III. RESULTS AND DISCUSSION

AFM images of HoSi_{2-x} nanowires on vicinal $\text{Si}(001)$ substrates with varying incoming flux are shown in Fig. 1. The observed nanowire width is limited by the resolution of the AFM tip and therefore appears much wider in the AFM image than the actual nanowire width. The deposition rate was 0.15 ML/min and the coverage was approximately 0.15 ML on the sample seen in Fig. 1(a). The mean nanowire length was measured as $0.5 \mu\text{m}$. When the growth rate was decreased to 0.02 ML/min, as seen in Fig. 1(b), the mean nanowire length increased to $2 \mu\text{m}$. Nanowires growth appears to be favored over nucleation at this growth rate and substrate temperature. In order to produce nanowire arrays with a high density and wire lengths exceeding $1 \mu\text{m}$, interrupted growth was employed. The growth rate was approximately 0.05 ML/min and the growth progressed for 2 minutes and was stopped and restarted. This was repeated 2 times. The total coverage was 0.35 ML and the mean nanowire length is slightly over $1 \mu\text{m}$. From these AFM images it can be deduced that at low growth rates nanowire nuclei primarily form when the flux is turned on and after this growth dominates over nucleation for the system of HoSi_{2-x} nanowires on $\text{Si}(001)$. The regime in which nanowire growth dominates over nucleation quite possibly varies with the type of rare earth metal. In the early stage of growth, the type of surface reconstruction metal atoms form on the Si surface prior to the disilicide reaction is dependent on the type of rare earth metal as is the coverage observed when nanowire nucleation takes place. For instance, Sm atoms form a 3×2 surface reconstruction and nanowire nucleation takes place at a coverage near 0.5 ML.[8] In comparison, Dy atoms form a 4×2 surface reconstruction and nanowires begin to nucleate at a coverage closer to 0.3 ML.[10]

STM images of ErSi_{2-x} , DySi_{2-x} , and SmSi_{2-x} nanowires are shown in Fig. 2 to demonstrate the dependence of nanowire width on large lattice mismatch. The lattice mismatch between $\text{Si} [\bar{1}10]$ $\{\text{Si}[110]\}$ and ErSi_{2-x} , DySi_{2-x} , and SmSi_{2-x} $[0001]$ $\{[11\bar{2}0]\}$ is 6.3% $\{-1.6\%$, and 7.6% $\{-0.1\%$, and 9.8% and $\{1.6\%$, respectively. The width of the ErSi_{2-x} nanowire, seen in Fig. 2(a), has a measured value of 4.7 nm and the height was measured as 0.7 nm . Shown in Fig. 2(b), the DySi_{2-x} nanowires have a measured average width of 2 nm , a measured height of 1 nm , and the average distance between the nanowires is 9 nm . In comparison, the SmSi_{2-x} nanowires,

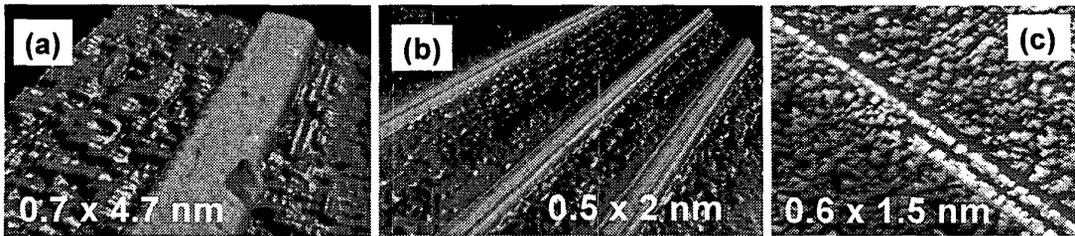


Figure 2: High-resolution STM images of (a) ErSi_{2-x} nanowires with wire width of 4.7 nm and height of 0.7 nm, (b) DySi_{2-x} nanowires: width is 2 nm and height is 1 nm, (c) SmSi_{2-x} nanowires: wire width is 1.5 nm and height is 0.7 nm.

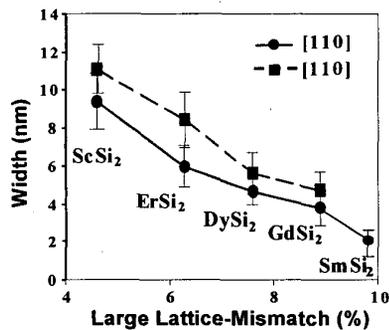


Figure 3: Variation of nanowire width as a function of mismatch between $\text{Si}[\bar{1}10]$ and $\text{RSi}_{2-x} [0001]$.

shown in Fig.2 (c), have an average measured width of 1.5 nm and a height of approximately 0.6 nm. In agreement with previous work,[6] the nanowire width decreases with increasing lattice mismatch between the $\text{Si}[\bar{1}10]$ and $\text{RSi}_{2-x} [0001]$ lattice constants. The graph in Fig. 3 demonstrates the monotonic decrease in nanowire width with increasing lattice mismatch along $\text{Si}[\bar{1}10]$.

Since the nanowire width is a function of the lattice mismatch between $[0001]$ and $\text{Si}[\bar{1}10]$, the formation of a ternary alloy of two rare earth metals and Si $\{(\text{R}_{1-y}\text{R}^*_y)\text{Si}_{2-x}\}$ may allow the tuning of nanowire width and improve the crystal quality of the nanowires. In view of small differences in the atomic size of many of the rare earth metals, one could expect that continuous solid solutions for many of the ternary rare earth metal disilicides exist at high temperatures. High resolution X-ray diffraction of $(\text{Er}_{1-y}\text{Gd}_y)\text{Si}_{2-x}$ and $(\text{Er}_{1-y}\text{Sm}_y)\text{Si}_{2-x}$ confirm the formation of two such solid solutions and demonstrate that the lattice parameter varies according to Vegard's Law.[9] Considering differing thermal expansion coefficients at the growth temperature of RSi_{2-x} nanowires on $\text{Si}(001)$, the $[11\bar{2}0]$ lattice constants of $(\text{Er}_{1-y}\text{Dy}_y)\text{Si}_{2-x}$ and $(\text{Er}_{1-y}\text{Ho}_y)\text{Si}_{2-x}$ alloys should closely match $a_{\text{Si}[\bar{1}10]}$. When evaporating solid solutions of $\text{Er}_{0.52}\text{Ho}_{0.48}$ and $\text{Er}_{0.85}\text{Dy}_{0.15}$ on $\text{Si}(001)$ vicinal substrates, nanowires did form on the surface. An AFM image of $(\text{Er}_{1-y}\text{Ho}_y)\text{Si}_{2-x}$ nanowires is shown in Fig. 4(a) In Fig. 4(b), a STM image of $(\text{Er}_{1-y}\text{Dy}_y)\text{Si}_{2-x}$ nanowires is shown. The nanowires are in the early stage of nucleation; the mean length is on the order of 100 nm. Both non-reacted metal and nanowires are visible on the surface as seen in the $40 \times 40 \text{ nm}^2$ STM image shown in Fig. 4(c). By examining this high resolution STM image, the mean nanowire width is measured as approximately 2 nm. The mean nanowire

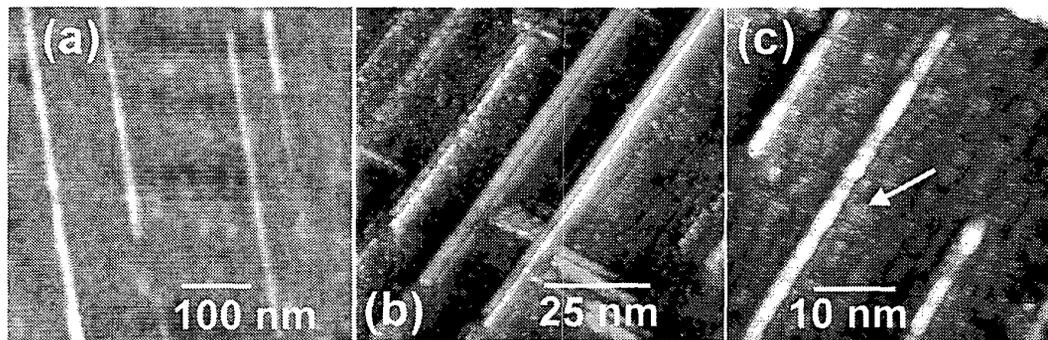


Figure 4: (a) AFM image of $(\text{Er}_{1-y}\text{Ho}_y)\text{Si}_{2-x}$ nanowires on a $\text{Si}(001)$ vicinal substrate. (b) STM image of $(\text{Er}_{1-y}\text{Dy}_y)\text{Si}_{2-x}$ nanowires on a $\text{Si}(001)$ vicinal substrate. The maximum nanowire length is approximately 200 nm. (c) High resolution STM image of $(\text{Er}_{1-y}\text{Dy}_y)\text{Si}_{2-x}$ nanowires seen in (b). The average measured width of the nanowires is approximately 2 nm. The arrow points to a region where non-reacted metal is visible on the surface.

width is close to that measured for pure Dy. An estimate of the composition of nanowires is $(\text{Er}_{0.25}\text{Dy}_{0.75})\text{Si}_{2-x}$ by taking into account the composition of the $\text{Er}_{0.85}\text{Dy}_{0.15}$ binary solid solution in the crucible and assuming an ideal solution to determine the effect of the differing vapor pressures for Er and Dy under the deposition conditions. AES, with a spot size on the order of a mm, of the Si surface and the $(\text{Er}_{1-y}\text{Dy}_y)\text{Si}_{2-x}$ nanowires detects Auger electrons characteristic of both Er and Dy on the surface. More quantitative AES analysis is necessary to confirm the nanowire composition.

IV. CONCLUSION

We have grown ordered arrays of ErSi_{2-x} , SmSi_{2-x} , DySi_{2-x} and HoSi_{2-x} nanowires oriented along Si[110] on Si(001) vicinal substrates with a miscut of 2.5° toward [110]. The nanowire width was shown to be a function of the lattice mismatch between Si $[\bar{1}10]$ and RSi_{2-x} [0001]. In the case of HoSi_{2-x} , interrupted growth produced dense arrays of nanowires with lengths exceeding 1 μm . To further improve crystal quality and tune the nanowire width, we explored the fabrication of ternary disilicide alloys. $(\text{Er}_{1-y}\text{Ho}_y)\text{Si}_{2-x}$ and $(\text{Er}_{1-y}\text{Dy}_y)\text{Si}_{2-x}$ nanowires have been grown on Si(001) vicinal substrates to investigate this possibility.

ACKNOWLEDGMENT

The authors acknowledge the Defense Advanced Research Projects Agency and the National Science Foundation (under a

GOALI grant no. NSF-DMR-0097621) in the United States for partial financial support of this project.

REFERENCES

- [1] J. A. Knapp and S. T. Picraux, *Appl. Phys. Lett.* **48**, 466 (1986).
- [2] H. W. Yeom, S. Takeda, E. Rotenberg, I. Matsuda, K. Schafer, C. M. Lee, S. D. Kevan, T. Ohta, T. Nagoa, and S. Hasegawa, *Phys. Rev. Lett.* **82**, 4898 (1999).
- [3] J. M. Luttinger, *J. Math. Phys.* **4**, 1154 (1963).
- [4] C. Preinesberger, S. Vandré, T. Kalka, and M. Dähne-Prietsch, *J. Phys. D* **31**, L43 (1998).
- [5] Y. Chen, D. A. A. Ohlberg, G. Medeiros-Ribeiro, Y. A. Chang, and R. S. Williams, *Appl. Phys. Lett.* **76**, 4004 (2000).
- [6] Y. Chen, D. A. A. Ohlberg, and R. S. Williams, *J. Appl. Phys.* **91**, 3213 (2002).
- [7] J. Nogami, B. Z. Liu, M. V. Katkov, C. Ohbuchi, and N. O. Birge, *Phys. Rev. B* **63**, 233305 (2001).
- [8] R. Ragan, Y. Chen, D. A. A. Ohlberg, G. Medeiros-Ribeiro, and R. S. Williams, *J. Cryst. Growth* **251**, 657 (2003).
- [9] M. Huang, J. Yang, Y. A. Chang, R. Ragan, Y. Chen, and R. S. Williams, unpublished results (2003).
- [10] B. Z. Liu and J. Nogami, *Surf. Sci.* **488**, 399 (2001).